

Hybrid Quantum-Classical Approach to Quantum Optimal Control

Jun Li,^{1,*} Xiaodong Yang,² Xinhua Peng,^{2,3,†} and Chang-Pu Sun¹

¹*Beijing Computational Science Research Center, Beijing 100193, China*

²*Hefei National Laboratory for Physical Sciences at Microscale and Department of Modern Physics, University of Science and Technology of China, Hefei, Anhui 230026, China*

³*Synergetic Innovation Centre of Quantum Information & Quantum Physics, University of Science and Technology of China, Hefei, Anhui 230026, China*

A central challenge in quantum computing is to identify more computational problems for which utilization of quantum resources can offer significant speedup. Here, we propose a hybrid quantum-classical scheme to tackle the quantum optimal control problem. We show that the most computationally demanding part of gradient-based algorithms, namely computing the fitness function and its gradient for a control input, can be accomplished by the process of evolution and measurement on a quantum simulator. By posing queries to and receiving messages from the quantum simulator, classical computing devices update the control parameters until an optimal control solution is found. To demonstrate the quantum-classical scheme in experiment, we use a nine-spin nuclear magnetic resonance system, on which we have succeeded in preparing a seven-correlated quantum state without involving classical computation of the large Hilbert space evolution.

PACS numbers: 03.67.Lx, 76.60.-k, 03.65.Yz

Quantum computing promises to deliver a new level of computation power [1]. Enormous efforts have been made in exploring the possible ways of using quantum resources to speed up computation. While the fabrication of a full-scale universal quantum computer remains a huge technical challenge [2], special-purpose quantum simulation can be an alternative [3–5]. Quantum simulators are designed to imitate specific quantum systems of interest, and are expected to provide significant speed-up over their classical counterparts [6]. Quantum simulation has found important applications for a great variety of computational tasks, such as solving linear equations [7, 8], simulating condensed-matter systems [9], calculating molecular properties [10, 11] and certifying untrusted quantum devices [12]. However, in view of experimental implementation, most of the proposed algorithms have hardware requirements still far beyond the capability of near-term quantum devices.

Recent advances towards building a modest-sized quantum computer have led to emerging interest in a quantum-classical hybrid approach [13–15]. The underlying idea is that by letting a quantum simulator work in conjunction with a classical computer, even minimal quantum resources could be made useful. In hybrid quantum-classical computation, the computationally expensive calculations, which yet might consume many qubits, are performed on a classical computer, whereas the difficult part of the computation is accomplished on a quantum simulator. The major benefit of this hybrid strategy is that it gives rise to a setup that can have much less stringent hardware requirements.

In this Letter, we propose a hybrid quantum-classical method for solving the quantum optimal control problem. Normally, the problem is formulated as follows: given a quantum control system and a fitness function

that measures the quality of control, the goal is to find a control that can achieve optimal performance. The importance of the problem lies in its extraordinarily wide range of applications in physics and chemistry [16]. However, current numerical approaches suffer from the scalability issue as they involve computation of the many time propagations of the state of the controlled system, which can be infeasible on classical computers for systems of large dimensions [17]. To address this computational challenge, we develop quantum versions of gradient-based optimal control algorithms [18]. We show that, given a reliable quantum simulator that efficiently simulates the controlled quantum evolution, then under reasonable conditions this simulator can be used to efficiently estimate both the fitness function and its gradient. Additionally, a classical computer is employed to store the control parameters as well as to determine the search direction in each iteration according to the gradient information that it receives from the simulator. Working in such a quantum-classical manner, there can be expected a significant saving of memory cost and time cost and hence an enhancement of the ability of solving the quantum optimal control problem for large-size quantum systems.

The proposed hybrid scheme is amenable to experimental implementation with current state-of-the-art quantum technology. Here, we also report a first experimental realization of our scheme on a nuclear magnetic resonance (NMR) system. The experimental results confirmed the feasibility of our method and show excellent performance in obtaining high-quality optimal control solutions.

Theory.—To start, we briefly describe the quantum state engineering problem. Consider an n -spin-1/2 quantum spin system, which evolves under a local Hamiltonian $H_S = \sum_l^L H_l$. Here each of the L terms H_l

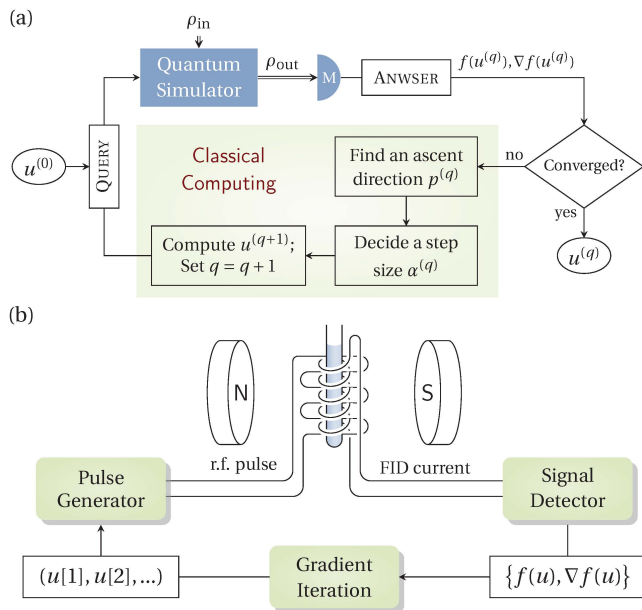


FIG. 1. (a) Hybrid quantum-classical approach to gradient-based optimal control iterative algorithms, wherein the quantum simulator is combined with classical computing devices to jointly implement the procedure of optimal control searching. Here, ρ_{in} is input state, ρ_{out} is output state, double-lined arrows signify quantum information, and M represents quantum measurement. (b) Schematic diagram of an NMR based implementation of the quantum-classical hybrid optimal control searching. The sample consists of an ensemble of spins and serves as a quantum processor. Query is encoded in input radio-frequency (r.f.) control pulse and the answer that the sample generates is extracted from observing the free induction decay (FID).

acts on a subsystem containing at most a constant number of spins. Such form of Hamiltonian can be efficiently simulated [19] and can describe a variety of quantum systems, e.g., quantum Ising model and Heisenberg model. Suppose the system is manipulated with a transverse time-varying magnetic control field $u(t) = (u_x(t), u_y(t)) : t \in [0, T]$. Let σ_x , σ_y and σ_z denote the Pauli operators, then the control Hamiltonian reads $H_C(t) = \sum_{k=1}^n (u_x(t)\sigma_x^k + u_y(t)\sigma_y^k)$, in which \hbar is set as 1 and the gyromagnetic ratios are not written explicitly. The control task is to steer the system between states of interest in the Liouvillian space. Normally, we define a fitness function to give a performance metric of the control. To this end, a set of operators $\mathcal{P}_n = \{P_k\}_{k=0}^{4^n-1} = \{I, \sigma_x, \sigma_y, \sigma_z\}^{\otimes n}$, with I being the 2×2 identity, is introduced. It constitutes an orthonormal basis of the state space: $\text{Tr}(P_k P_j) / 2^n = \delta_{kj}$ for $k, j = 0, \dots, 4^n - 1$. Thus any state can be represented as a vector with respect to \mathcal{P}_n . Let the system's starting point be ρ_i and the target be $\bar{\rho} = \sum_{s \in S} x_s P_s$ where S is the index set for s . As we are considering closed system engineering, ρ_i should be unitarily convertible to $\bar{\rho}$.

Now the state-to-state transfer task is formulated as the quantum optimal control problem [18]:

$$\begin{aligned} \max \quad & f(U(T)\rho_i U(T)^\dagger, \bar{\rho}) = \text{Tr}(U(T)\rho_i U(T)^\dagger \cdot \bar{\rho}) / 2^n, \\ \text{s.t.} \quad & \dot{U}(t) = -i \left[H_S + \sum_{k=1}^n (u_x(t)\sigma_x^k + u_y(t)\sigma_y^k) \right] U(t), \end{aligned}$$

where $U(0) = I^{\otimes n}$ and f , the fitness function, is expressed as a functional of the input control $u(t)$ and may possess many local extrema. Except for relatively small systems with two or three qubits [20, 21], analytically solving the problem for generic H_S is difficult.

Generally one must resort to numerical investigations, and the most favored approach is to employ gradient-based optimization methods. A gradient-based algorithm generates a sequence of iterates $u^{(0)}, u^{(1)}, \dots$, which starts from a designed trial input or even simply a random guess, and stops when a certain termination condition is fulfilled [22]. The move from one iterate $u^{(q)}$ ($q \geq 0$) to the next follows the line search strategy

$$u^{(q+1)} = u^{(q)} + \alpha^{(q)} p^{(q)}, \quad (1)$$

that is, it first fixes a search direction $p^{(q)}$ and then identifies a move distance $\alpha^{(q)}$ along that direction. The computation of $p^{(q)}$ makes use of information about f and the gradient ∇f at current iterate $u^{(q)}$, and possibly also information from earlier iterates. The step size $\alpha^{(q)}$ is chosen such that a sufficient increase in f can be acquired. The algorithm succeeds if the sequence $f(u^{(0)}), f(u^{(1)}), \dots$ converges to a desired local extremum. There exist various types of gradient-based algorithms, which are classified based on the method used for determining the search direction. For example, the known gradient ascent pulse engineering (GRAPE) [18] algorithm finds local extrema by taking steps proportional to the gradient, while conjugated gradient [23] and quasi-Newton methods [24] would search along other gradient-related directions that allow for faster convergence speed.

Here we develop a hybrid quantum-classical framework for gradient-based optimal control. It would be convenient to cast the ideas in terms of the standard oracle-based optimization model [25, 26]. Consider an oracle function $\mathcal{O} : u \rightarrow \{f(u), \nabla f(u)\}$ which, when queried at any point u , gives the corresponding value of f and ∇f . Obviously that constructing such an oracle \mathcal{O} represents the most computationally resource-consuming part of the optimization procedure, and we propose to realize it with using a reliable quantum simulator. The simulator does not necessarily have to be universal. For instance, it can just be provided by the controlled system itself [27]. The simulator works with a classical computer which stores the control variables, and if necessary records all iterative information. Our hybrid scheme consists of successive rounds of control updates, see Fig. 1. For each round the classical computer first sends the current point u to

the oracle \mathcal{O} as input meaning that it is posing a query, and then according to the answer of \mathcal{O} it executes a line search subroutine so as to decide at which point the next query should be made. Here, the query is encoded in control pulse and the answer is extracted through quantum measurements on the final state of the simulator.

So far we have not mentioned the convergence properties of the optimization. Gradient-based algorithms may get trapped at suboptimal points. Yet researches show that, under certain conditions most of the control landscapes are trap free and convergence to an optimal solution is usually fast [28]. In our hybrid quantum-classical scheme, the only change is that we use quantum resources to implement the oracle function \mathcal{O} . Therefore, the convergence properties will remain unchanged as long as our quantum simulator is sufficiently trustable.

Now we explain how the oracle \mathcal{O} is quantumly constructed. We use the number of experiments needed to compute \mathcal{O} as a complexity measure of the method. Running the numerical optimization requires that the control field be discretized. Let the pulse $u(t)$ be divided into M slices with each time slice being of constant magnitude and fixed length $\tau = T/M$. In consideration of memory cost, M should be polynomially scaled. The m -th slice control $u[m]$ generates the propagator

$$U_m = \exp \left\{ -i \left[H_S + \sum_{k=1}^n (u_x[m] \sigma_x^k + u_y[m] \sigma_y^k) \right] \tau \right\}.$$

For notational brevity let $U_{m_2}^{m_1}$ denote $U_{m_2} \cdots U_{m_1+1} U_{m_1}$ where $m_2 \geq m_1$. So the final state is $\rho_f = U_1^M \rho_i U_1^{M\dagger}$. We hence have the following expression for f

$$f = \text{Tr}(\rho_f \bar{\rho}) / 2^n = \sum_{s \in S} x_s \text{Tr}(\rho_f P_s) / 2^n. \quad (2)$$

It can be readily seen from the equation that, rather than full tomography of final state, f can be directly measured with $|S|$ experiments. That is, for the s -th experiment we first initialize our simulator at ρ_i , then simulate the system evolution under control u and then measure the final state with basis operator P_s . After this we sum up all the measurement results according to Eq. (2) and hence obtain an estimation of f .

Next let us see how to compute the $2M$ -dimensional gradient vector $g = \nabla f = (g_x[m], g_y[m])$, where $g_\alpha[m] = \partial f / \partial u_\alpha[m]$ ($\alpha = x$ or y). To first order approximation, it is evaluated as [18]

$$g_\alpha[m] = \sum_{k=1}^n \text{Tr} \left(-i \tau U_{m+1}^M \left[\sigma_\alpha^k, U_1^m \rho_i U_1^{m\dagger} \right] U_{m+1}^M \dagger \bar{\rho} \right) / 2^n. \quad (3)$$

The approximation is good if τ is sufficiently small. Note that for any operator ρ , there is

$$[\sigma_\alpha^k, \rho] = i \left[R_\alpha^k \left(\frac{\pi}{2} \right) \rho R_\alpha^k \left(\frac{\pi}{2} \right)^\dagger - R_\alpha^k \left(-\frac{\pi}{2} \right) \rho R_\alpha^k \left(-\frac{\pi}{2} \right)^\dagger \right], \quad (4)$$

in which $R_\alpha^k(\pm\pi/2)$ is the $\pm\pi/2$ rotation about α axis on the k -th qubit. The essential point is that we can compute the commutator by means of local qubit rotations. Substituting the formula into g ,

$$g_\alpha[m] = \frac{\tau}{2} \sum_{k=1}^n \left[\text{Tr} \left(\rho_{\alpha+}^{km} \bar{\rho} \right) - \text{Tr} \left(\rho_{\alpha-}^{km} \bar{\rho} \right) \right] / 2^n, \quad (5)$$

where $\rho_{\alpha\pm}^{km} = U_{m+1}^M R_\alpha^k(\pm\pi/2) U_1^m \rho_i (U_{m+1}^M R_\alpha^k(\pm\pi/2) U_1^m)^\dagger$. Therefore, to obtain the m -th component of g_α , we perform $2n$ experiments: we (i) sequentially take out an element from the operation set $\{R_\alpha^k(\pm\pi/2)\}_{k=1,\dots,n}$, and insert it after the m -th slice evolution; (ii) measure the distances of the final states with respect to $\bar{\rho}$ and (iii) combine all the measurement results according to Eq. (5). A quick calculation shows that in each round of iteration in total $4nM|S|$ experiments are needed to perform gradient estimation.

Summarizing the above derivations, we conclude that in total we need to perform $(4nM + 1)|S|$ experiments on the quantum simulator to estimate f and g . It is interesting to seek for instances for which our scheme can be qualitatively advantageous over conventional approaches. Obviously that target states possessing exponential number of nonzero components require also that many measurements to take. This implies that, to ensure the whole process be feasible, we have to restrict consideration to specific kind of target states. An important fact in quantum computing says that, to build up quantum operations out of a small set of elementary gates is generically inefficient [1]. In other words, there are overwhelmingly many states that are complex in the sense that they take exponential size of quantum circuit to approximate. Therefore, it makes sense if we restrict to relatively less complicated states, for example those which admit sparse representation with respect to some basis, where the basis fulfils the condition that measurement of any its element consumes only polynomial resources. In present setting, we will be interested in $|S|$ -sparse states under basis \mathcal{P}_n with $|S| \ll |\mathcal{P}_n|$. Despite of the problem simplification, from the practical side they are undoubtedly still difficult tasks at current level of large-system control technology. Sparsity assumption drastically reduces the time cost for physically implementing \mathcal{O} and in consequence the great chance of our oracle machine model to provide significant speedup.

Experiment.—We chose the fully ^{13}C -labeled crotonic acid as our test system, on which we demonstrated the idea of using the sample to compute its own optimal control pulse. Fig. 2(a) shows the molecular structure of the sample. The four carbon nuclei plus the five proton nuclei constitute a nine-spin system, in which the methyl protons H_3 , H_4 and H_5 are chemically and magnetically equivalent and hence are indistinguishable. Experiment is carried on a Bruker Avance III 400 MHz spectrometer at room temperature. The system Hamiltonian takes the

form: $H_S = \sum_{k=1}^n \Omega_k \sigma_z^k / 2 + \pi \sum_{k < j}^n J_{kj} \sigma_z^k \sigma_z^j / 2$, where Ω_k is the precession frequency of the k -th spin, and J_{kj} is the coupling between the k -th and j -th spin, see supplementary material [29] for their values. To describe states of the nuclei, we use deviation density matrices, that is, the traceless part of the density matrices up to an overall scale [30]. Our goal is to create the seven-correlated state $\bar{\rho} = \sigma_z^1 \sigma_z^2 \sigma_z^3 \sigma_z^5 \sigma_z^7 \sigma_z^8 \sigma_z^9$, which is the largest multiple-correlated operator that can be directly observed from the spectrum. Observation is made on C_2 because all the couplings are adequately resolved. Our experiment is divided into two parts: reset and preparation.

In the reset part we reset the system to a fixed initial state ρ_i , which has to be unitarily equivalent to $\bar{\rho}$. So the system's equilibrium state is not considered because it has different spectra with that of $\bar{\rho}$. Although there are many candidates, we choose $\rho_i \propto \sigma_z^2$ for convenience of observation and design a corresponding initialization procedure, see Fig. 2(b). First, we apply a continuous wave (cw) on the proton channel. Because of the steady state hetero-nuclear Overhauser effect (NOE) [31], provided that the cw irradiation is sufficiently long and strong, then the system will be driven asymptotically into a steady state ρ_{ss} of the form: $\rho_{ss} = \sum_{k=1}^4 \epsilon_{ss}^k \sigma_z^k$, that is, the protons are saturated. In experiment, the irradiation is set to be 10 s of duration and 2500 Hz of magnitude. As expected we see the establishment of the steady state, in which only the carbons' polarizations are left, but with enhanced bias compared to the equilibrium state. For example, the boost factor of C_2 is about 1.8. Next, we retain just the signal of C_2 by first rotate the polarizations of other carbons to the transverse plane and then destroy them with z axis gradient field. This gives the desired initial state ρ_i .

The preparation part aims to steer ρ_i towards $\bar{\rho}$. To give a good initial control guess to accelerate convergence, we designed an approximate preparation circuit. The approximate circuit is constructed based on a simplified system Hamiltonian which ignores the small couplings and the small differences between large couplings of the original Hamiltonian. Such simplification manifests which couplings are allowed to evolve for preparing $\bar{\rho}$ thus enables direct circuit construction, see Fig. 2(b). The circuit thus constructed, if we turn back to the real Hamiltonian, generates a final state that deviates $\bar{\rho}$ only slightly: $f \approx 0.9824$. Moreover, the circuit length is 16.36 ms, much shorter than system's relaxation time, so the preparation stage can be taken as unitary. In order that the number of control parameters after pulse discretization be as few as possible, we adopt relatively large time step length $\tau = 20 \mu\text{s}$. We use Gaussian shaped selective pulses to implement the rotational gates. Each selective pulse has its pulse-width determined according to which qubit it is acting on. Excluding the free J evolutions, we have in total 2×108 nonzero pulse parameters to be optimized. We have employed a compilation procedure

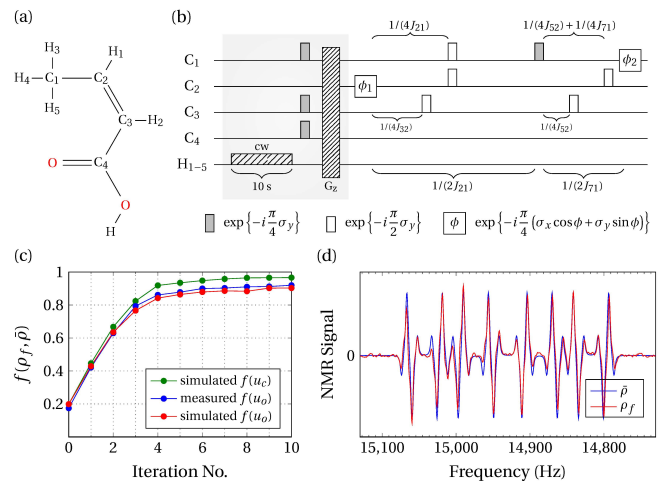


FIG. 2. (a) Molecular structure of crotonic acid. (b) Pulse sequence scheme for our multiple-quantum coherence generation experiment. The grey part is designed to reset the system back into ρ_i , and the preparation part is an approximate circuit (in which cw: continuous wave; G_z : gradient pulse along z axis; $\phi_1 = -18^\circ$ and $\phi_2 = 82^\circ$) aimed for making the transform $\rho_i \rightarrow \bar{\rho}$. (c) Iterative results for our system. Here u_c and u_o denote the controls obtained by searching on a classical computer and on the sample respectively. (d) NMR spectrum of ρ_f after 10 times of iteration under the observation of C_2 . It is placed with the simulated ideal spectrum of target state $\bar{\rho}$ together for comparison.

[32, 33] to systematically reduce the errors that come in when the ideal rotational operations are implemented through soft selective pulses, yet f still drops severely. Therefore, some extent of pulse optimization is necessary.

We add a small amount of random disturbances to the above constructed selective pulse network. The purpose of doing so is to start the oracle iteration from a relatively low-quality control and hence to witness a more notable rising of f . According to our previous analysis, we roughly figure out the experiment time cost for each round of iteration to be about 5 hours. We have demonstrated the query action on the sample for 10 times. Fig. 2(c-d) shows the experimental results, from which we see clearly that the successively updated pulse is indeed approaching a solution of the optimal control problem. Because that measurement inaccuracies induce errors in gradient estimation, it is as expected that some degree of deviation of the experimental growth of f from that performed on a classical computer appears. Therefore, the important challenge left open is to understand quantitatively that how measurement inaccuracies affect the convergence efficiency.

Discussion.—From the control theory perspective, the apparatus in our experiment, including a control input generator, a sample of molecules and a measurement device, interact as a closed learning loop. In each cycle of the loop, the fitness information learned from the sam-

ple directs the optimization to achieve a given control objective. Such strategy has the advantage of reliability and robustness. Learning algorithm is the crucial ingredient, and previous studies have been mainly focused on using stochastic searching strategies such as evolutionary algorithms [34, 35]. We here have shown that a large class of gradient-based methods can also be incorporated into the closed loop learning control model. This will be important for realizing high-fidelity quantum control experiments, such as is needed in the fields of quantum information processing and spectroscopy.

Future work will seek to gain a better understanding of the feasibility of the hybrid quantum-classical approach to quantum optimal control. NMR is an excellent platform on which to test various quantum control methods, but for our scheme its drawback is the relatively long reset (relaxation) time. It can be envisioned that on some other quantum information processing candidate systems that are with much shorter operation time and relaxation time [2], the search process may get several orders of magnitude faster. We expect the methodology developed in this work can promote studies of scalable quantum controls on larger quantum systems.

This work is supported by the National Basic Research Program of China (973 Program, Grant No. 2014CB921403), the National Key Research and Development Program (Grant No. 2016YFA0301201), the Foundation for Innovative Research Groups of the National Natural Science Foundation of China (Grant No. 11421063), the Major Program of the National Natural Science Foundation of China (Grant No. 11534002), the State Key Development Program for Basic Research of China (Grant Nos. 2014CB848700 and 2013CB921800), the National Science Fund for Distinguished Young Scholars (Grant No. 11425523), and the National Natural Science Foundation of China (Grant No. 11375167 and Grant No. 11605005).

* lijunwu@mail.ustc.edu.cn

† xhpeng@ustc.edu.cn

- [1] M. A. Nielsen and I. L. Chuang, *Quantum Computation and Quantum Information* (Cambridge University Press, Cambridge, 2000).
- [2] T. D. Ladd, F. Jelezko, R. Laflamme, Y. Nakamura, C. Monroe, and J. L. O'Brien, *Nature (London)* **464**, 45 (2010).
- [3] A. M. Childs and W. van Dam, *Rev. Mod. Phys.* **82**, 1 (2010).
- [4] J. I. Cirac and P. Zoller, *Nat. Phys.* **8**, 264 (2012).
- [5] P. Hauke, F. M. Cucchietti, L. Tagliacozzo, I. Deutsch, and M. Lewenstein, *Rep. Prog. Phys.* **75** 082401 (2012).
- [6] R. P. Feynman, *Int. J. Theor. Phys.* **21**, 467 (1982).
- [7] A. W. Harrow, A. Hassidim, and S. Lloyd, *Phys. Rev. Lett.* **103**, 150502 (2009).
- [8] A. M. Childs, *Nat. Phys.* **5**, 861 (2009).
- [9] G. A. Álvarez, D. Suter, and R. Kaiser, *Science*, **349**, 846 (2015).
- [10] B. P. Lanyon *et al.*, *Nat. Chem.* **2**, 106 (2010).
- [11] P. J. J. O'Malley *et al.*, *Phys. Rev. X* **6**, 031007 (2016).
- [12] N. Wiebe, C. Granade, C. Ferrie, and D. G. Cory, *Phys. Rev. Lett.* **112**, 190501 (2014).
- [13] J. R. McClean, J. Romero, R. Babbush, and A. Aspuru-Guzik, *New J. Phys.* **18**, 023023 (2016).
- [14] B. Bauer, D. Wecker, A. J. Millis, M. B. Hastings, and M. Troyer, *Phys. Rev. X* **6**, 031045 (2016).
- [15] S. Bravyi, G. Smith, and J. A. Smolin, *Phys. Rev. X* **6**, 021043 (2016).
- [16] C. Brif, R. Chakrabarti, and H. Rabitz, *New J. Phys.* **12**, 075008 (2010).
- [17] H. J. Hogben, M. Krzystyniak, G. T. P. Charnock, P. J. Hore, and I. Kuprov, *J. Magn. Reson.* **208**, 179 (2011).
- [18] N. Khaneja *et al.*, *J. Magn. Reson.* **172**, 296 (2005).
- [19] S. Lloyd, *Science* **273**, 1073 (1996).
- [20] N. Khaneja, R. Brockett, and S. J. Glaser, *Phys. Rev. A* **63**, 032308 (2001).
- [21] A. Carlini, A. Hosoya, T. Koike, and Y. Okudaira, *Phys. Rev. A* **75**, 042308 (2007).
- [22] J. Nocedal and S. J. Wright, *Numerical Optimization* (Springer, New York, 2006).
- [23] A. Borzi, J. Salomon, and S. Volkwein, *J. Comput. Appl. Math.* **216**, 170 (2008).
- [24] P. de Fouquieres, S. G. Schirmer, S. J. Glaser, and I. Kuprov, *J. Magn. Reson.* **212**, 412 (2011).
- [25] A. S. Nemirovski and D. B. Yudin, *Problem Complexity and Method Efficiency in Optimization* (Wiley, New York, 1983).
- [26] Y. Nesterov, *Introductory Lectures on Convex Optimization: Basic Course*. (Springer-Verlag, 2004).
- [27] C. Ferrie and O. Moussa, *Phys. Rev. A* **91**, 052306 (2015).
- [28] A. N. Pechen and D. J. Tannor, *Phys. Rev. Lett.* **106**, 120402 (2011).
- [29] See Supplemental Material for more details.
- [30] O. W. Sørensen, G. W. Eich, M. H. Levitt, G. Bodenhausen, and R. R. Ernst, *Prog. Nucl. Magn. Reson. Spectrosc.* **16**, 163 (1983).
- [31] M. H. Levitt, *Spin Dynamics: Basics of Nuclear Magnetic Resonance* (John Wiley & Sons Ltd, England, 2008).
- [32] C. A. Ryan, C. Negrevergne, M. Laforest, E. Knill, and R. Laflamme, *Phys. Rev. A* **78**, 012328 (2008).
- [33] J. Li, J. Cui, R. Laflamme, and X. Peng, *Phys. Rev. A* **94**, 032316 (2016).
- [34] H. Rabitz, R. de Vivie-Riedle, M. Motzkus, K. Kompa, *Science* **288**, 824 (2000).
- [35] R. S. Judson and H. Rabitz, *Phys. Rev. Lett.* **68**, 1500 (1992).

**SUPPLEMENTARY MATERIAL:
“HYBRID QUANTUM-CLASSICAL APPROACH TO QUANTUM OPTIMAL CONTROL”**

GRADIENT-BASED METHODS

Our aim is to develop a hybrid quantum-classical framework for gradient-based optimal control. As we have described in the main text, a gradient-based iterative algorithm generates successive iterates from an initial guess $u^{(0)}$, where the move from one iterate $u^{(q)}$ to the next $u^{(q+1)}$ consists of the following steps:

- (1) compute $\mathcal{O} : u^{(q)} \rightarrow \{f(u^{(q)}), \nabla f(u^{(q)})\}$,
- (2) determine a gradient-related search direction $p^{(q)}$,
- (3) find an optimal step size

$$\alpha^{(q)} = \arg \max_{\alpha} f(u^{(q)} + \alpha p^{(q)}),$$

- (4) update $u^{(q+1)} = u^{(q)} + \alpha^{(q)} p^{(q)}$.

We have shown that step (1) can be done with using a quantum simulator. Step (3) is a one-dimensional search. Often, the step size need not be determined exactly. Inexact search may be performed in a number of ways, such as a backtracking line search or using the Wolfe conditions. They can be done by a classical computer. Now we take a closer look at how step (2) is accomplished using the hybrid quantum-classical setup.

Different types of gradient-based algorithms use different strategies to compute the search direction. Representative gradient-based algorithms include gradient ascent, conjugate gradient and quasi-Newton methods [1].

Gradient ascent. The gradient ascent method simply takes steps along the gradient.

$$p^{(q)} = \nabla f(u^{(q)}). \quad (6)$$

Nonlinear conjugate gradient ascent. In numerical optimization, nonlinear conjugate gradient method is a widely used method for solving nonlinear optimization problems. The search direction is determined by

$$p^{(q)} = \nabla f(u^{(q)}) - \beta^{(q)} p^{(q-1)}, \quad (7)$$

where $\beta^{(q)}$ is computed according to Fletcher-Reeves formula

$$\beta^{(q)} = \frac{(\nabla f(u^{(q)}))^T \nabla f(u^{(q)})}{(\nabla f(u^{(q-1)}))^T \nabla f(u^{(q-1)})},$$

or Polak-Ribière formula:

$$\beta^{(q)} = \frac{(\nabla f(u^{(q)}))^T (\nabla f(u^{(q)}) - \nabla f(u^{(q-1)}))}{(\nabla f(u^{(q-1)}))^T \nabla f(u^{(q-1)})},$$

or some other formulas such as Hestenes-Stiefel formula.

Quasi-Newton method. Quasi-Newton methods also require only the gradient of the fitness function to be supplied. They are able to produce superlinear convergence by utilizing information about the changes in gradients. The search direction is determined by

$$p^{(q)} = H^{(q)} \nabla f(u^{(q)}), \quad (8)$$

where $H^{(q)}$ is an approximation to the Hessian, and is also updated in each iteration. There exist a number of different methods for updating $H^{(q)}$ [1]. For example, the Davidon-Fletcher-Powell formula goes

$$H^{(q+1)} = H^{(q)} + \frac{\Delta u^{(q)} (\Delta u^{(q)})^T}{(\Delta u^{(q)})^T y^{(q)}} - \frac{H^{(q)} y^{(q)} (y^{(q)})^T H^{(q)}}{(y^{(q)})^T H^{(q)} y^{(q)}},$$

and the Broyden-Fletcher-Goldfarb-Shanno formula goes

$$H^{(q+1)} = \left(I - \frac{\Delta u^{(q)} (y^{(q)})^T}{(y^{(q)})^T \Delta u^{(q)}} \right) H^{(q)} \left(I - \frac{y^{(q)} (\Delta u^{(q)})^T}{(y^{(q)})^T \Delta u^{(q)}} \right) + \frac{\Delta u^{(q)} (\Delta u^{(q)})^T}{(y^{(q)})^T \Delta u^{(q)}},$$

where $\Delta u^{(q)} = u^{(q+1)} - u^{(q)}$, $y^{(q)} = \nabla f(u^{(q+1)}) - \nabla f(u^{(q)})$ and the initial $H^{(0)}$ can be set as the identity matrix.

We can see from Eqs. (6–8) that, in their quantum-classical hybrid implementation, the classical computer should have recorded all iterative information. In computing the search direction $p^{(q)}$, the classical computer would use information about f and ∇f at current iterate, and possibly also information from earlier iterates.

EXPERIMENT

In this section, we give more details of how our experiment is performed. Our experimental system is the fully ^{13}C -labeled crotonic acid. The system parameters are given in Fig. 3(a). What we want to demonstrate in experiment is the process of using this sample to compute its own optimal control pulse. Concretely, we choose to study the following state-to-state transfer task:

$$\rho_i = \sigma_z^2 \rightarrow \bar{\rho} = \sigma_z^1 \sigma_z^2 \sigma_z^3 \sigma_z^5 \sigma_z^7 \sigma_z^8 \sigma_z^9. \quad (9)$$

As we have described in the main text, the implementation of the hybrid quantum-classical algorithm requires repeatedly querying the sample. Each query action is composed of three stages: initialization, preparation and detection. The final detection of $\bar{\rho}$ is made by observing the spectrum of C_2 , see Fig. for the ideal spectrum. We shall not consider errors present in the initialization and detection step, nor the relaxation effects during the preparation step.

Initialization

The initialization step aims to create the initial state ρ_i from the equilibrium state

$$\rho_{eq} = \sum_{k=1}^4 \epsilon_{eq} \sigma_z^k + 4 \sum_{k=5}^9 \epsilon_{eq} \sigma_z^k \rightarrow \rho_i = \sigma_z^2, \quad (10)$$

where ϵ_{eq} is the equilibrium polarization magnitude of carbon. This is accomplished through a non-unitary process, which utilizes the steady state hetero-nuclear Overhauser effect as explained in the main text. The system at ② is $\rho_{ss} = \sum_{k=1}^4 \epsilon_{ss}^k \sigma_z^k$ where ϵ_{ss}^k denotes the steady state polarization magnitude. The system at ③ is $\rho_i = \epsilon_{ss}^2 \sigma_z^2$. From experiment, we have obtained that $\epsilon_{ss}^2 \approx 1.8 \epsilon_{eq}^2$. For convenience, from here on we shall rescale ϵ_{ss}^2 as 1.

Note that there is a more familiar way of producing pure operator σ_z^2 , namely selectively rotate all the spins except C_2 and followed a longitudinal gradient pulse. However, our method here has two important advantages, both attributed to NOE: (i) higher polarization of initial state, hence an increased signal-to-noise ratio of the spectrum; (ii) faster reset time, NOE takes much less time to reset the system, that for our sample this is found to be about six times faster. Therefore, NOE based reset procedure greatly reduces the total time cost of our experiment.

Preparation

Constructing an approximate circuit. Firstly, we construct an ideal preparation circuit for an approximate Hamiltonian, which of course would be an approximate circuit for the real Hamiltonian. Consider a simplified coupling network as given in Fig. 3(b). Let us denote the approximate Hamiltonian out of this simplified coupling network as \hat{H}_S . Based on the simplified Hamiltonian, we build up an ideal circuit that is able to realize the desired state-to-state transfer with perfect fidelity, see Fig. 3(c). The circuit proceeds in two sub-steps: in the first sub-step, we first turn σ_z^2 into 1-coherence and then generate three-correlated operators $\sigma_z^1 \sigma_x^2 \sigma_z^3$ and $\sigma_z^1 \sigma_y^2 \sigma_z^3$ through coupled evolutions of J_{12} and J_{23} ; in the second sub-step, we first add a $\pi/2$ rotation about y axis to the first spin and then generate seven-correlated operator $\sigma_z^1 \sigma_x^2 \sigma_z^3 \sigma_z^5 \sigma_z^7 \sigma_z^8 \sigma_z^9$ through coupled evolutions of J_{17} , J_{18} , J_{19} and J_{25} . Here, in each sub-step, the unwanted J coupling evolutions should be appropriately refocused. Back to the real Hamiltonian H_S , this circuit generates a final state with high fidelity $f = 0.9824$, see Fig. 4.

Selective pulse sequence compilation. Next, we seek to construct a pulse sequence that can implement the approximate circuit. The circuit is composed of multiple-spin rotational gates and free evolutions. To realize the rotational gates, we take use of frequency selective pulses.

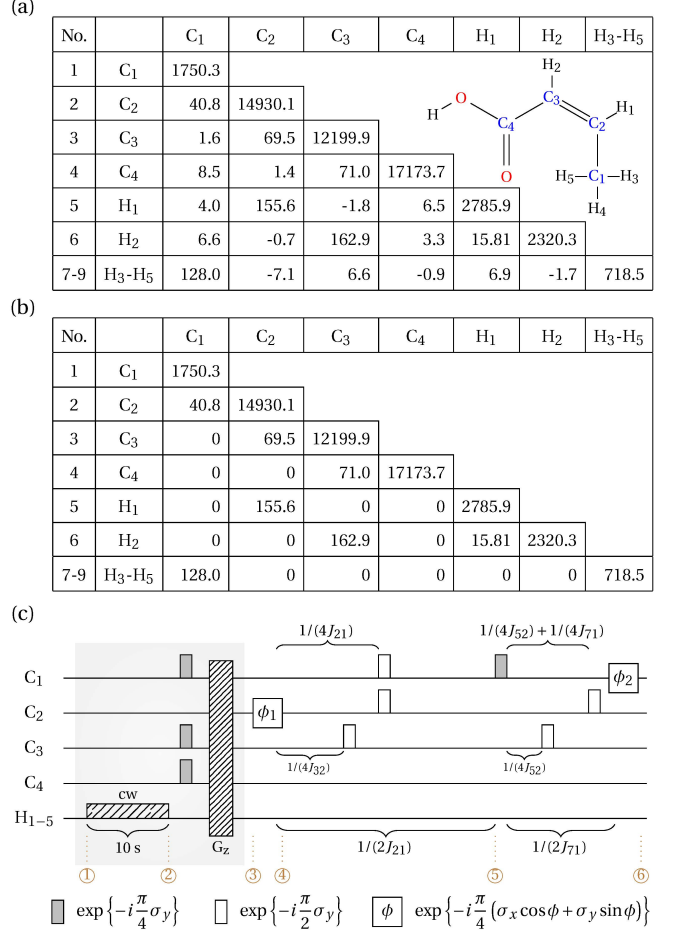


FIG. 3. (a) The Hamiltonian parameters (all in Hz) are experimentally determined on a 400 MHz spectrometer. In the table, diagonal elements give chemical shifts with respect to the base frequency for carbon and proton transmitters; off-diagonal elements give J coupling terms. (b) Simplified coupling network. It is obtained by ignoring the small couplings and the small differences between large couplings of the original Hamiltonian. (c) Operation sequence for our state-to-state optimal control experiment.

Selective pulses have the property of selectively exciting spins over a limited frequency region, while minimizing influences to spins that are outside this region. For example, a rotational gate on a specific spin can be realized by a rotating Gaussian that is on resonance with that spin. The approximate circuit contains in total 7 multiple-spin rotations, each implemented through a selective pulse with the basic Gaussian selective pulse shape. The time lengths of these selective pulses are not all the same, actually they are determined according to the frequency distances of the spins to be excited with the other spins.

In order that the number of control parameters after pulse discretization be as few as possible, we adopt relatively large time step length $\tau = 20 \mu\text{s}$. Accordingly the time lengths of the selective pulses and the free evolutions of the pulse sequence are not exactly the same as

State	Approximate circuit for \tilde{H}_S	Approximate circuit for H_S	Compiled pulse sequence for H_S
③	σ_z^2	σ_z^2	σ_z^2
④	$-0.3090\sigma_x^2 - 0.9511\sigma_y^2$	$-0.3090\sigma_x^2 - 0.9511\sigma_y^2$	$-0.3016\sigma_x^2 - 0.9509\sigma_y^2 + \dots$
⑤	$-0.3090\sigma_z^1\sigma_x^2\sigma_z^3 + 0.9511\sigma_z^1\sigma_y^2\sigma_z^3$	$-0.3090\sigma_z^1\sigma_x^2\sigma_z^3 + 0.9511\sigma_z^1\sigma_y^2\sigma_z^3$	$-0.0395\sigma_z^1\sigma_x^2\sigma_z^3 + 0.9712\sigma_z^1\sigma_y^2\sigma_z^3 + \dots$
⑥	$\sigma_z^1\sigma_x^2\sigma_z^3\sigma_z^5\sigma_z^7\sigma_z^8\sigma_z^9$	$0.9823\sigma_z^1\sigma_x^2\sigma_z^3\sigma_z^5\sigma_z^7\sigma_z^8\sigma_z^9 + \dots$	$0.9358\sigma_z^1\sigma_x^2\sigma_z^3\sigma_z^5\sigma_z^7\sigma_z^8\sigma_z^9 + \dots$

FIG. 4. State evolution of the quantum system under the constructed quantum circuit and the compiled selective pulse sequence.

those in the circuit of Fig. 3(c), and they are redefined as such: $t \rightarrow \tau \text{Round}(t/\tau)$ where t represents any of $1/(4J_{21}), 1/(4J_{32}), 1/(2J_{21}), \dots$. The resulting pulse is of length 16.36 ms, discretized into 818 time slices and of which in total 108 slices are nonzero. Therefore, there are 2×108 nonzero pulse parameters to optimize.

It is important to be aware of that a selective pulse just approximately implements the target operation. Various types of errors arise when transferring a circuit directly into a selective pulse sequence without correction. And as the number of gates contained in the circuit grows large, the error accumulation will become increasingly serious. To address this problem, Refs. [2, 3] put forward a pulse sequence compilation program. The compilation program systematically adjusts the pulse parameters of an arbitrary input selective pulse sequence so that errors up to first-order can be corrected. The compilation procedure is efficient. With application of the compilation method to our pulse sequence, the control accuracy is greatly improved, see the compiled results shown in Fig. 4. Although the compilation program can not eliminate all control imperfections that higher-order errors still exist, it is quite useful in that, the pulse sequence after compilation is of relatively high fidelity and can be used as a good starting point for subsequent gradient-based optimization. We refer the reader to Ref. [2] for a detailed elaboration of how to take both pulse compilation

method and optimal control method together as a basis to pulse design in large-sized quantum system control.

Time cost of the oracle function \mathcal{O} . As we have derived in the main text, it requires $(4nM + 1)|S|$ experiments to be performed on the sample to calculate the function $\mathcal{O} : u \rightarrow (f(u), g(u))$. The time cost of each experiment is composed of three parts: (i) the time cost of initialization, which we now denote by T_0 ; (ii) the time cost of running the circuit, which is 16.36 ms; (iii) the time cost of detection, which takes 1~2 seconds.

For our NMR experiments, we could let the sample freely relax back to its equilibrium state ρ_i , which takes about 5 times the relaxation characteristic time of the spins, i.e., about 60 s. However, our initialization is performed in another approach as is described in the main text, and in doing so, the reset process could be six times faster. Therefore, our experimental time cost of the oracle function \mathcal{O} is reduced to 5 hours.

* lijunwu@mail.ustc.edu.cn

† xhpeng@ustc.edu.cn

- [1] J. Nocedal and S. J. Wright, *Numerical Optimization* (Springer, New York, 2006).
- [2] C. A. Ryan, C. Negrevergne, M. Laforest, E. Knill, and R. Laflamme, Phys. Rev. A **78**, 012328 (2008).
- [3] J. Li, J. Cui, R. Laflamme, and X. Peng, Phys. Rev. A **94**, 032316 (2016).